Tip-Tilt Mirror Control in Gravitational Fabry-Perot Interferometer Cavity

Roel van Silfhout
Nikhef Mechanic Technologies
Roelvsilfhout@outlook.com

ABSTRACT

Gravitational wave detection is achieved by a Fabry-Perot Michelson interferometer, which measures the change in arm length when the wave causes a strain in space-time. Optical components, such as the mirrors in the cavity, must be precisely controlled to measure these strains in the arms. This paper outlines a method for controlling the position of a suspended mirror by actuating voice coils with a breakout box which is driven by a control loop program and measuring the position of the mirror with shadow sensors in 3 degrees of freedom: forward (called the X direction), pitch and yaw.

Keywords

Gravitational wave, Michelson interferometer, General Relativity, Tip-Tilt Mirror Control

INTRODUCTION

The general theory of relativity published in 1916 by Albert Einstein, revolutionized our view of the universe and predicted the existence of gravitational radiation. Such radiation is generated by the acceleration of mass-energy distributions and is expected to behave like a wave-like distortion in space-time propagating at the speed of light. Propagating gravitational waves change the curvature of four-dimensional space-time and can change the measured separation between free masses. Interferometers can be considered suited to the direct detection of gravitational waves because the setup is in principle simple and can be built on a larger scale. If free test-masses were attached to the end mirrors, then a gravitational wave of the correct polarization passing through the instrument, would create an optical path difference between orthogonal arms of the interferometer, which can be measured. Nowadays, gravitational wave detection plays an important role in physics, which is evident from the number of detectors. VIRGO (Variability of solar IRradiance and Gravity Oscillations) is only gravitational wave detector in Europe, which is a collaboration between 6 countries. In the Netherlands, Nikhef (National Institute for nuclear physics and High-Energy Physics) as a research institute plays the largest role in this collaboration.

However, in order for the detector to work on these large scales it has to be resistant to vibrations, noise or other outside influences. In specific, my research involves the realization and commissioning of a small scale tabletop fully suspended Fabry-Perot Michelson interferometer, with the following research question: What is the mechanical characteristic of the tip-tilt mirrors suspension and how can it be controlled? This setup will make use of LabVIEW software and hardware when measuring and actuating the system in a closed loop. The goal of the setup is to test and validate control noise reduction techniques before introducing them in the real detector at Virgo.

THEORY

An important principle related to general relativity is the concept that light bends in a gravitational field. Masses positioned between a distant light source and a detector could of bend light from the source as the light travels towards the detector. Since gravitation and acceleration are equivalent, acceleration of a light beam should produce the same effect, which was the result of Einstein's elevator experiment. These phenomena are explained by the fact that mass bends space-time. Space-time is a combination of space and time as a set of coordinates, which has four dimensions. The curvature of space-time bends the light around the mass because light moves along the shortest path in space-time. Mass in acceleration generates changes in space-time continuum, which vibrates like a wave at the speed of light. These propagating waves are called gravitational waves, which transport energy in a wave-form similar to electromagnetic radiation as photons. When a gravitational wave is observed, it shows that the space-time medium is changed by the effects of strain [1,2].

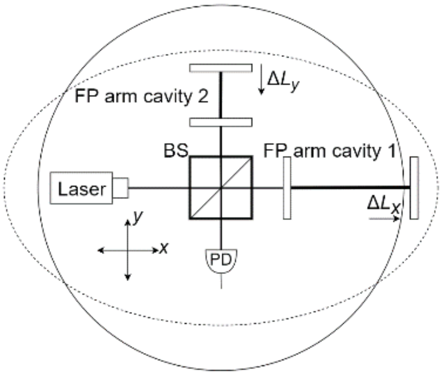

Figure 1: Fabry-Perot Michelson interferometer where the optical path length changes due to + polarization propagating gravitational wave.

SRC 2019, December 5, 2019, The Netherlands.

Michelson interferometer

Strain is an important quantity since it directly relates to the accumulated phase which is measured by laser interferometric GW observatories. Extra phase $\Delta\varphi$ accumulated by a photon that travels down and back the arm of a laser interferometer in the presence of a GW is:

$$\Delta\varphi = \frac{4\pi\Delta L}{\lambda} \tag{1}$$

Where λ is the photon's wavelength and ΔL is the difference in distance moved between the end mirrors relative to the beam splitter. When light is generated in the laser and it propagates towards the beam splitter, the partially reflecting beam splitter will divide the beam into two other beams, and the paths from the beam splitter to the mirrors are called the arms of the interferometer. Light reflects back to the beam splitter and recombines the 2 beams back in the beam splitter. This interferometer setup can then measure the difference in arm length, because the phase changes over distance and a different phase means that the beam resulting from the beam interference changes [3,4,5].

METHOD

In order to realize a small scale fully suspended interferometer, that will make use of real-time software and hardware to test and validate novel control noise reduction techniques, tip-tilt mirrors are used to function as a beam splitter and as cavity arm mirrors in the optical setup. The tip-tilt mirror suspension is controlled by a closed-loop system in which the NOSEMs are responsible for the positioning of the optical components in the interferometer. NOSEM (Nikhef Optical Sensor and Electro-Magnetic actuator) is a system which measures the position of a flag, attached to the optics. Position of the flag is controlled by the voice coil actuators, who exercise a force on a magnet inside the flag. Four of the actuators control the suspended mirror in 3 degrees of freedom total. Simultaneously, the position of these flags is determined by shadow sensors. Where the displacement of the flag along the longitudinal axis changes the proportion of the collimated beam from the LED that is incident upon the photodiode. The scheme incorporates a mask with a slit and a collimating lens to the emitter assembly. The lens improves the collimation of the emission from the LED, the mask ensures only paraxial rays contribute to the noise floor.

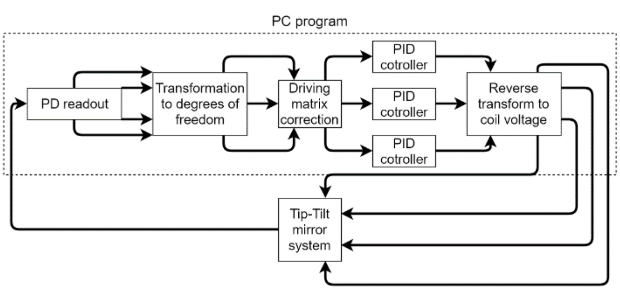

Figure 2: Tip-tilt mirror control block diagram.

To actuate the coils and measure the flag position electronics are used to power the LED, convert the relative low photodiode current to a determinable voltage, and control the coil current with the output voltage which originates from the DAC. The circuit board is connected to a 7 V source which can generate a current up to 5 A in order to actuate the voice coils. Software controls the NOSEMs with a DAC and ADC (digital to analog and analog to digital converter), which is a closed loop system.

Control system

A LabVIEW program measures the position of each flag, and uses the shadow sensor responses of each NOSEM to convert the raw data to distances. In the beginning of the program the output voltages of the individual NOSEMs are measured and converted into positions. In order to convert these values into the positions in the different degrees of freedom, a sensing matrix is used. Where after each position is controlled individually by a PID controller. The resulting signal is fed back into the voice coils by reverse transforming with the sensing matrix

Measurements

The goal of the first set of measurements is to characterize the shadow sensors in the NOSEMs and the electronics that come with it. This paper only focuses on the shadow detector response, to determine their linear range (see the original thesis for all the different measurements such as noise, frequency response and drift). NOSEM measurements were done with a stage on which the flag was attached. The stage was then driven by a LabVIEW program and measured the photodiode voltage output at the same time. It can be controlled in the longitudinal direction to characterize the shadow detector from the origin of the stage (0 mm) to 4.5 mm in the direction of the NOSEM. Determining the driving matrix is done by a different LabVIEW program. The matrix is obtained by applying a ramp voltage or a low-frequency signal (typically 0.1 Hz) in the linear region separately for the 3 degrees of freedom and measuring the distance each flag travels in all 4 NOSEM's for each measurement. To determine the correction for the degrees of freedom when the mirror is moved, the average change (or amplitude of a sine signal) of all the directions is determined while the coils move the mirror in one direction. This is repeated for all dimensions and includes the sensitivity of all shadow sensors. Finally, when the position in the 3 degrees of freedom is controlled, the transfer function and the impulse response can be determined. The impulse response gives information about the damping amplitude while controlling the position and how the system can be corrected [6].

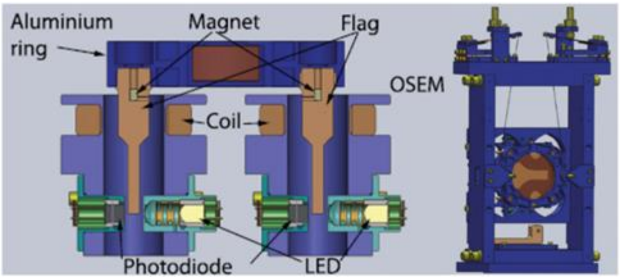

Figure 3: A cross-section of the NOSEMs with the corresponding flags and besides the whole tip-tilt mirror [6].

By applying the NOSEMs to the tip-tilt mirror, the mechanical system can be characterized. A schematic of the suspension is shown in figure 3. Four flags are attached to each side of the mirror. The resonance frequencies of these 6 degrees (where 3 are controlled) of freedom are designed and modeled to be below 10 Hz, which are with the application of gravitational wave detection at relatively low frequencies. D-Pitch and d-Yaw distances are chosen so that the resonance frequencies are approximately 1 Hz, but slightly different in order to distinguish between the degrees of freedom, which also applies to the x-direction. The actuation magnets that are controlled by the voice coils (with a resistance of 27 Ω) in the NOSEMs are positioned at the end of the flags which are attached to the ring surrounding the mirror.

RESULTS

When applying the NOSEMs in the control system of the tip-tilt mirror it is important to know what the output voltage of each NOSEM is a function of the flag position, shown in figure 4. The average linear range of the NOSEMs is 0.73 ± 0.01 mm.

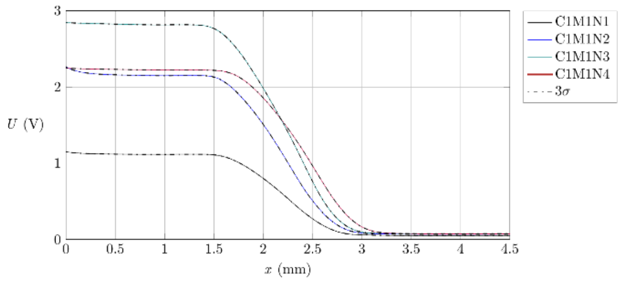

Figure 4: Output voltage as a function of the flag position relative to the NOSEM for all shadow sensors for mirror 1.

When the flag approaches the beam from the LED, the proportion of the beam that is incident on the photodiode decreases. This can be explained by the geometry of the LED, where most light originates from the middle of the LED, and because the surface of the LED is circular, change in the area which the flag cover is the lowest at the ends of the circle shaped beam. Which is equivalent to the light power incident on the flag. This effect causes a Gaussian distribution of photons in the beam. So the rate at which the voltage drops at the beginning of the beam is almost 0, then the voltage decreases faster until it reaches the middle of the beam. After the middle point, the voltage drops slower until the flag covers the whole beam. However, the sensitivity is different for each sensor.

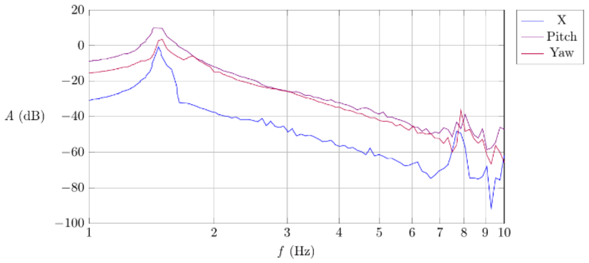

Figure 5: Transfer function when driving the four NOSEM coils and reading out the shadow sensors.

Transfer function

The transfer function and the phase of the system are measured by a dynamic signal analyzer. This machine uses a frequency sweep input signal to determine the response while measuring the input and output signal of the tip-tilt mirror system. The transfer function in the 3 degrees of freedom is shown in figure 5. Figure 5 confirms that the resonance frequency in the 3 degrees of freedom is around 1.5 Hz in specific: X is 1.425 ± 0.005 Hz, the pitch 1.430 ± 0.005 Hz, and the yaw is 1.500 ± 0.005 Hz. These resonance frequencies are relatively close by design because the system has to be damped in all directions when the mirror is controlled.

Control response

A PID controller can be configured by first measured the impulse response of the system, without controlling the position, and applying the driving matrix. Figure 6 shows the data of the response in the X direction.

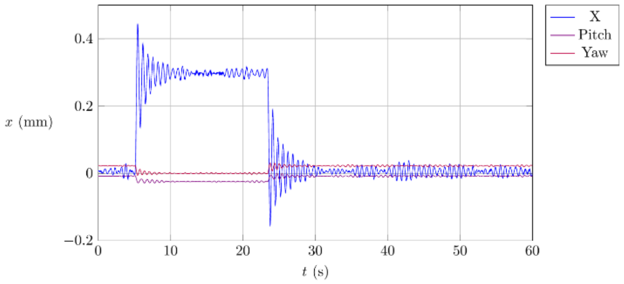

Figure 6: Impulse response in the X-direction without controlling the position.

It can be concluded that impulse response amplitude is too big to control the position in the X direction. The pitching of the PID controller results in the following impulse response shown in figure 7.

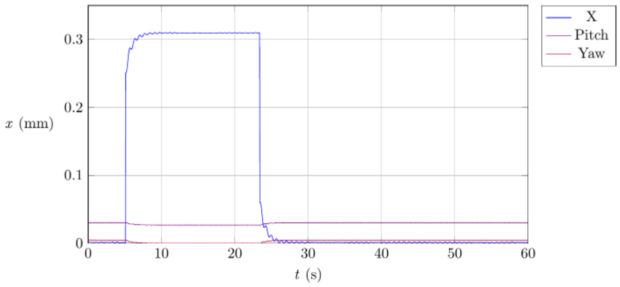

Figure 7: Impulse response in the X-direction while controlling the position with the tuned PID controller.

The response amplitude of the X, pitch, and yaw direction are reduced by: 0.287 mm, 0.228 mm, and 0.275 mm respectively. In conclusion, the PID controller can drive the NOSEMs, but there is still a slight fluctuation of the position. Note that the impulse response was done over the linear range from the middle to the end, but uncontrolled the response goes slightly beyond the linear range.

CONCLUSION

Position of the tip-tilt mirror is derived by the shadow of 4 different flags, attached to each corner of the mirror, cast on the shadow sensors. From the characteristics in figure 4 can be concluded that the beam geometry incident on the photodiode causes a Gaussian characteristic (with an error in the order of 10 mV). Results also show that each NOSEM has a different shadow sensor sensitivity, that has to be corrected by the program when controlling the mirror with the sensors and actuators. These sensors can be used for the tip-tilt mirror control, because they meet the requirement of a minimum range of 0.7 mm. The data shown in figure 4 proves that the expected deviation is not showing in the characteristics when the NOSEMs are measured. It is possible to control the tip-tilt mirror in real-time by applying 4 NOSEM to actuate and measure in 3 degrees of freedom. The resonance frequencies in the degrees of freedom are relatively close, but not exactly the same to prevent total resonance of the system. Controlling the position of the mirror is achieved with a PID (proportional–integral–derivative) controller closed loop system. Actuation of the system is corrected by a driving matrix, which gives information about the voltage required to move a certain amount in a specific degree of freedom. This matrix is measured by a separate program, with a voltage ramp in the 3 degrees of freedom. The consequences of these improvements and results are that my programs could be applied to the cavity mirrors of the interferometer, which could assist further research in improving the gravitational wave detector. If these improvements can continue it can later be applied in the real detector.

ROLE OF THE STUDENT

My role in this project as an undergraduate student was to assist in the development of a table top gravitational wave interferometer for VIRGO. In specific the work revolved around the electronics powering the detector and the programming of the positioning software in LabVIEW under the supervision of Rob Walet. The products of this project by the student were the LabVIEW programs to do the mentioned measurements and control the tip-tilt mirror. The tip-tilt mirror itself is designed and produced by the supervisor.

REFERENCES

1. Einstein, A. "Lens-like Action of a Star by the Deviation of Light in the Gravitational Field", *Science*, (1936), 506–507.
2. Heavens, A. "General Relativity", http://star-www.st-and.ac.uk/~hz4/gr/HeavensGR.pdf.
3. Carroll, S. M. "Weak fields and gravitational radiation", *University of Chicago*, December (1997), https://ned.ipac.caltech.edu/level5/March01/Carroll3/Carroll6.html.
4. Flannagan, E., Hughes, S., "The basics of gravitational wave theory", *Department of Physics and Center for Space Research*, Cambridge, (2005).
5. "Physics of LIGO Lecture 3", *LIGO*, https://labcit.ligo.caltech.edu/~ajw/LIGO_SURF02_3.pdf.
6. Slagmolen, B. J. J., Mullavey, A. J., Miller, J., McClelland, D. E., Fritschel, P., "Tip-Tilt Mirror Suspension: Beam Steering for Advanced LIGO Sensing and Control Signals", *LIGO*, Cambridge, (2011).